

9-2018

Moderate Heat Application Enhances the Efficacy of Nanosecond Pulse Stimulation for the Treatment of Squamous Cell Carcinoma

Chelsea M. Edelblute
Old Dominion University

Sigi Guo
Old Dominion University, s2guo@odu.edu

Embo Yang
Old Dominion University

Chunqi Jiang
Old Dominion University, cjiang@odu.edu

Karl Schoenbach
Old Dominion University, kschoenb@odu.edu

See next page for additional authors

Follow this and additional works at: https://digitalcommons.odu.edu/bioelectrics_pubs

 Part of the [Biomedical Commons](#), [Biomedical Engineering and Bioengineering Commons](#), [Biotechnology Commons](#), and the [Oncology Commons](#)

Repository Citation

Edelblute, Chelsea M.; Guo, Sigi; Yang, Embo; Jiang, Chunqi; Schoenbach, Karl; and Heller, Richard, "Moderate Heat Application Enhances the Efficacy of Nanosecond Pulse Stimulation for the Treatment of Squamous Cell Carcinoma" (2018). *Bioelectrics Publications*. 219.
https://digitalcommons.odu.edu/bioelectrics_pubs/219


Original Publication Citation


Edelblute, C. M., Guo, S., Hornef, J., Yang, E., Jiang, C., Schoenbach, K., & Heller, R. (2018). Moderate heat application enhances the efficacy of nanosecond pulse stimulation for the treatment of squamous cell carcinoma. *Technology in Cancer Research & Treatment*, 17, 1-9. doi:10.1177/1533033818802305

Authors

Chelsea M. Edelblute, Sigi Guo, Embo Yang, Chunqi Jiang, Karl Schoenbach, and Richard Heller

Moderate Heat Application Enhances the Efficacy of Nanosecond Pulse Stimulation for the Treatment of Squamous Cell Carcinoma

Technology in Cancer Research & Treatment
Volume 17: 1-9
© The Author(s) 2018
Article reuse guidelines:
sagepub.com/journals-permissions
DOI: 10.1177/1533033818802305
journals.sagepub.com/home/tct


Chelsea M. Edelblute, MS¹, Siqi Guo, MD¹, James Hornef, MS^{1,2},
Enbo Yang, PhD¹, Chunqi Jiang, PhD^{1,2},
Karl Schoenbach, Dr. rer. nat.^{1,3}, and Richard Heller, PhD^{1,3} 

Abstract

Nanosecond pulse stimulation as a tumor ablation therapy has been studied for the treatment of various carcinomas in animal models and has shown a significant survival benefit. In the current study, we found that moderate heating at 43°C for 2 minutes significantly enhanced *in vitro* nanosecond pulse stimulation-induced cell death of KLN205 murine squamous cell carcinoma cells by 2.43-fold at 600 V and by 2.32-fold at 900 V, as evidenced by propidium iodide uptake. Furthermore, the ablation zone in KLN205 cells placed in a 3-dimensional cell-culture model and pulsed at a voltage of 900 V at 43°C was 3 times larger than in cells exposed to nanosecond pulse stimulation at room temperature. Application of moderate heating alone did not cause cell death. A nanosecond pulse stimulation electrode with integrated controllable laser heating was developed to treat murine ectopic squamous cell carcinoma. With this innovative system, we were able to quickly heat and maintain the temperature of the target tumor at 43°C during nanosecond pulse stimulation. Nanosecond pulse stimulation with moderate heating was shown to significantly extend overall survival, delay tumor growth, and achieve a high rate of complete tumor regression. Moderate heating extended survival nearly 3-fold where median overall survival was 22 days for 9.8 kV without moderate heating and over 63 days for tumors pulsed with 600, 100 ns pulses at 5 Hz, at voltage of 9.8 kV with moderate heating. Median overall survival in the control groups was 24 and 31 days for mice with untreated tumors and tumors receiving moderate heat alone, respectively. Nearly 69% (11 of 16) of tumor-bearing mice treated with nanosecond pulse stimulation with moderate heating were tumor free at the completion of the study, whereas complete tumor regression was not observed in the control groups and in 9.8 kV without moderate heating. These results suggest moderate heating can reduce the necessary applied voltage for tumor ablation with nanosecond pulse stimulation.

Keywords

nanosecond pulse stimulation, nanosecond pulse electric field, electroporation, irreversible electroporation, ablation

Abbreviations

ANOVA, analysis of variance; DPBS, Dulbecco phosphate buffered saline; IRE, irreversible electroporation; MH, moderate heating; NPS, nanosecond pulse stimulation.

Received: March 22, 2018; Revised: June 21, 2018; Accepted: August 20, 2018.

Introduction

Squamous cell carcinomas are one of the most common types of ectodermal cancer. These cancers arise as a malignancy in renewable squamous epithelial cells in the skin, esophagus, lung, and cervix. Cutaneous squamous cell carcinoma is the second most common form of nonmelanoma skin cancer, accounting for an estimated 20% of all skin cancers, with its incidence

¹ Frank Reidy Research Center for Bioelectronics, Old Dominion University, Norfolk, VA, USA

² Department of Biomedical Engineering, College of Engineering, Old Dominion University, Norfolk, VA, USA

³ School of Medical Diagnostic & Translational Sciences, College of Health Sciences, Old Dominion University, Norfolk, VA, USA

Corresponding Author:

Richard Heller, PhD, Frank Reidy Research Center for Bioelectronics, Old Dominion University, 4211 Monarch Way, Suite 300, Norfolk, VA, USA.
Email: rheller@odu.edu



increasing among the aging population.¹ Moreover, squamous cell carcinomas make up 10% to 15% of all lung cancers.²

Irreversible electroporation (IRE) has recently emerged as a viable tool for cancer therapy, providing a minimally invasive treatment platform that is both tolerable and effective.³⁻⁵ As a nonthermal ablation technology, IRE has advantages over alternative therapies such as radiofrequency heating,⁶⁻⁸ cryotherapy, and hyperthermia,⁹ which are associated with high morbidity and mortality due to thermal damage to extracellular tissues and contiguous vital structures.¹⁰⁻¹³ However, local relapse due to incomplete ablation and clinical complications associated with IRE protocols and electrode needle placement¹⁴ limits its potential as a therapy.¹⁵⁻¹⁷ This limitation was congruent with increasing tumor size, where a larger tumor becomes more difficult to treat without complications.³

Current studies have extended IRE pulse protocols to the nanosecond range. Nanosecond pulse stimulation (NPS) has been shown to effect the barrier function not only on the extracellular cell membrane but also on the membrane of intracellular organelles.¹⁸⁻²⁰ These biological effects likely assist the killing action of short duration pulses. *In vivo*, NPS has been used for the treatment of murine melanoma,²¹ hepatocellular carcinoma in a rat,^{22,23} and murine squamous cell carcinoma.²⁴ Furthermore, in humans, NPS was effective for the treatment of basal cell carcinoma lesions.²⁵

The effect of temperature on cells and biological tissues has been well studied, where an increase in temperature yields an increase in cell permeability.^{26,27} This dilation can facilitate the transfer of otherwise impermeant deliverables, for example, plasmid DNA²⁸ or chemotherapeutics²⁹ to cells or tissues. When the application of heat and electric field is combined, these effects are more pronounced and delivery of extracellular molecules is more efficient.^{27,28} Additionally, a recent study demonstrated cooling cells on ice following nanosecond pulse exposure had a synergistic cytotoxic effect compared to cells moved to 37°C after NPS.³⁰

Our hypothesis is that a moderate increase in the temperature of the target tumor can sensitize the target tumor for NPS. We previously demonstrated the combination of moderate heat and IRE pulse protocols in an ectopic murine pancreatic adenocarcinoma model, where tumor impedance was reduced with the application of heat, and tumor regression and survival were improved.³¹ In the current study, we used 100 ns pulses in combination with controlled moderate heat from an infrared laser to ablate squamous cell carcinomas. To test this hypothesis, a 3-dimensional (3-D) agarose gel cell-culture model was studied for *in vitro* tumor ablation. Furthermore, the efficacy of moderate heating in combination with nanosecond pulse stimulation (MH-NPS) for tumor ablation was evaluated in an ectopic murine squamous cell carcinoma model.

Materials and Methods

3-D Cell Model

KLN205-ATCC CRL1453 (ATCC, Manassas, Virginia) mouse lung squamous cell carcinoma cells were maintained in culture

with a complete growth medium of Eagle minimal essential medium with 4 mM L-glutamine, supplemented with 10% heat-inactivated fetal bovine serum, and 5% penicillin/streptomycin. Cells were kept in a 37°C incubator supplied with 5% CO₂. Cells were tested for mycoplasma and confirmed negative.

A 3-D agarose cell-culture model was adopted for *in vitro* tumor ablation.^{31,32} Solutions of 1% and 2.5% low-gelling temperature agarose in complete media were prepared and kept at 37°C. A base layer of 900 µL 2.5% agarose was evenly poured on the bottom of a 3.5 cm plate avoiding bubbles. The plate was then chilled at 4°C until addition of the cell suspension. Briefly, 3×10^6 KLN205 cells were resuspended in 1 mL of 1% low-gelling agarose gently and overlaid on the 2.5% layer. The plate was immediately chilled at 4°C for 4 minutes to set, after which the 3-D cell models were incubated at 37°C for 20 minutes before applying the pulse protocol.

Nanosecond Pulse Stimulation in a 3-D Cell Model

Electric pulses were delivered to the 3-D model using a 2-needle electrode comprised of tungsten wires, with an electrode gap of 1 mm. Experimental groups included cells pulsed at ambient temperature and cells preheated to 43°C before pulse application. A heat block was used to reach and maintain 43°C. Temperature was monitored by a thermocouple inserted into the edge of the agarose for the duration of the protocol. Pulsing parameters were randomly selected so as to not bias one group from another. To indicate the location of pulsing, a permanent ink mark was made on the underside of the 3.5 cm plate to indicate the location of each individual site. Sites of pulse delivery were spaced such that one region would not overlap or interfere with another. In total, no more than 10 pulsing, heated, or no treatment sites were included on a single plate. Two hundred pulses of a 300 ns pulse duration, a pulse frequency of 50 Hz, and applied electric fields of 150, 300, 600, 750, and 900 V were used as the pulsing parameters. A sham control, where the electrode was inserted into the agarose without delivering pulses, and a heat-only control were included. Plates were returned to the incubator for 2 hours before assessing cell death.

Quantification of Cell Death

Two hours after pulsing, cells were stained with propidium iodide (4 µg/mL) to distinguish the live cells from the dead cells; $1 \times$ Dulbecco phosphate buffered saline (DPBS) was supplemented to each well for imaging. Immunofluorescence micrographs were taken on an Olympus IX71 fluorescent stereo microscope using an Olympus DP71 CCD camera (Olympus, Center Valley, Pennsylvania). The permanent ink mark was used as a guide under bright field to first locate individual sites, then the fluorescence filter was applied for visualizing cell death. All micrographs were taken at the same exposure conditions. Quantification of fluorescence signal was done using ImageJ software (Version 1.47). The integrated

fluorescence density was determined by drawing a region of interest around the area of fluorescence signal. The average integrated fluorescence density of 3 to 5 samples is reported (\pm standard deviation).

Determination of Ablation Zone

Fluorescence micrographs of pulsed cells for quantifying cell death were also used in determining the area of ablation using ImageJ software. A scale was set for each image using the 1 mm electrode gap as a guide. The center point of the 2 electrode imprints, that is, the areas void of cells, served as end points of the 1 mm scale. After setting the scale, a horizontal line was drawn from the center of the ellipse to the edge of increasing fluorescence intensity, encompassing the region with the highest propidium iodide uptake. This measurement served as the semi-major axis (mm). Similarly, a vertical line, perpendicular to the length, was drawn from the center of the ellipse to the edge of increasing fluorescence intensity, also encompassing the region with the highest propidium iodide uptake. This measurement served as the semi-minor axis (mm). The area of the ellipse-shaped ablation zone (mm^2) was calculated by multiplying the semi-major and semi-minor axes by π wherein $A = \pi ab$. The average of 3 to 5 samples is reported (\pm standard deviation).

Two Dimensional Electric Field Simulation of MH-NPS

To quantify the electric field distribution, 2 dimensional (2-D) numerical simulations were performed using the commercially available finite element method solver COMSOL Multiphysics (Version 5). A 2-D electrostatic model was created using experimental data from *in vitro* NPS with and without heating. We utilized data from our strongest NPS parameter, 900 V, at room temperature and 43°C for constructing the simulation. Using the electrode specifications of 2 tungsten wires measuring 0.25 mm in diameter and water as the substrate medium, an electric field diagram was created in the plane perpendicular to the needle electrodes. The electric field was mapped in color (V/m) and contoured (V) per the 1 mm electrode gap and applied electric field.

Murine Tumor Model

Female DBA/2 mice (6-8 weeks of age) were purchased from Jackson Laboratories (Bar Harbor, Maine). Mice were injected with 1×10^6 KLN205 cells in 50 μL (DPBS) subcutaneously on a preshaved left flank. A total of 50 mice were used for this experiment. The size of the primary tumor was assessed by digital calipers twice a week along with body weight and clinical observation of the animals. Tumor volume was determined using the following formula: $V = \pi ab^2/6$, where a is the longest diameter and b is the shortest diameter perpendicular to a . Mice were euthanized at the end of the follow-up period or when they met clinical criterion described at experimental end points, such as morbidity, or with a threshold tumor volume at or exceeding 1000 mm^3 . Mice that were tumor free at the

completion of the study were challenged on the opposite, right flank, with 5×10^5 KLN205 cells in 50 μL DPBS. This tumor volume was recorded. All experimental protocols were approved by the Old Dominion University Institutional Animal Care and Use Committee, and all experiments were performed in accordance with relevant guidelines and regulations.

Laser Heating and Control System

To achieve controlled heating and maintain a constant surface temperature of the treatment object at 43°C, a programmable and automatically adjustable heating system was designed. The heating system consists of a 980 nm wavelength infrared laser (Lasermate Group Inc, Walnut, California), whose optical emission can be modulated in time, an optical fiber that delivers the infrared laser light to the treatment surface, a thermopile (ZTP-135SR, Amphenol Advanced Sensors, St. Mary's, Pennsylvania) that serves as a temperature sensor for the irradiated surface, and a programmable control circuit providing laser modulation and the collected temperature information to a LabVIEW (2014) interface. The temperature of the target tissue was maintained by opening and closing the laser beam shutter, automatically controlled with an Arduino proportional–integral–derivative controller.

Electrode Design

A 4-needle 5 mm \times 7 mm rectangular array was utilized for MH-NPS to squamous cell carcinoma tumors. The laser fiber was secured in the center of the array, providing heat to the area within the applied electric field. The probe was encased in a Teflon cylinder. With this arrangement, a Gaussian distribution of the infrared irradiation was measured in an independent calibration study and the beam width was determined to be 2 mm (based on 10%-90% value). This complements the electric field strength distribution of the 4-needle array electrodes, which was illustrated and detailed in our previous work.³¹ A thermopile was included in the electrode configuration and positioned on the side at such an angle to accurately record the surface temperature at the site of the laser irradiation (Figure 1A). Individual sheaths of ethylene tetrafluoroethylene tubing were used to cover the shaft of each needle electrode, leaving just 3 mm of the electrode unsheathed or exposed (Figure 1B). This accommodated a safer placement of the electrode over the tumor, wherein the sheath served as a barrier to prevent the needles from being inserted too deeply into the animal, avoiding injury to the internal organs from needle placement. The sheathing also provided insulation between the needles and the thermopile, reducing local electrical breakdown from high-voltage noise.

Moderate Heating Nanosecond Pulse Stimulation of Tumors

Mice were anesthetized for MH-NPS. To anesthetize, animals were placed in an induction chamber infused with a mixture of 3% to 5% isoflurane and 97% oxygen gas for several minutes.

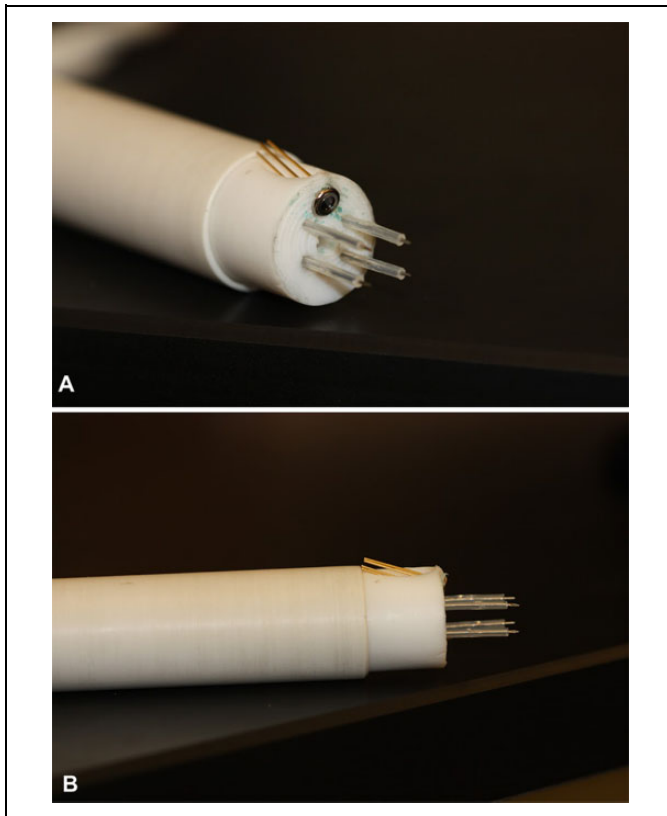


Figure 1. Electrode array for MH-NPS. Four-needle high-voltage electrodes are arranged in a 5 mm \times 7 mm array with center port for an infrared laser fiber. Thermopile for surface temperature monitoring is angled toward target (A). Ethylene tetrafluoroethylene tubing sheaths high-voltage needle electrodes leaving 3 mm exposed to insert into target tumor (B). MH-NPS indicates nanosecond pulse stimulation with moderate heating.

Once anesthetized, mice were fitted with a standard rodent mask supplied with 2% to 3% isoflurane and 97% to 98% oxygen to maintain a surgical plane of anesthesia. Excess fur was removed from the area surrounding the tumor before pulse application. Squamous cell carcinoma tumors were treated when they reached an average size of $\sim 50 \text{ mm}^3$, approximately 1 week after induction. A single ablative treatment was applied. The electrode was positioned to cover the entire area of tumor, with the needles inserted completely into the skin. The pulse parameters for ablation were 600, 100 ns pulses, at a frequency of 5 Hz. The experimental groups included 9.8 kV without heat, 9.8 kV with heat, 15.4 kV without heat, 15.4 kV with heat, and 21 kV without heat. Untreated tumors were included as a control group. In the heated tumors, the laser fiber was applied prior to delivering the pulses, and for the duration of the pulse protocol once the target temperature of 43°C was reached. A temperature of 43°C was maintained for the entirety of the pulse protocol. A heat-only control with no applied pulses was also included, where the tumor was preheated to 43°C and maintained at that temperature for the length of time required to complete the pulse protocol, that is, 2 minutes. After completion of treatment, each mouse was

monitored continuously until recovered from anesthesia, as indicated by their ability to maintain sternal recumbency and to exhibit purposeful movement.

Statistical Analysis

Statistical significance between groups in the 3-D cell model was determined using a 2-way analysis of variance (ANOVA) with a Tukey-Kramer multiple comparisons posttest. Results are expressed as the mean of 3 to 5 replicates per group (\pm standard deviation). Significant results were determined with respect to cells exposed to pulses at room temperature unless otherwise noted. A P value less than .05 was considered significant.

Statistical significance between the groups for the murine tumor model was determined by 2-way ANOVA with a Tukey-Kramer multiple comparisons test (GraphPad Prism Software, La Jolla, California). Results are expressed as the mean of 5 to 8 individual replicates per group (\pm standard deviation). Significant results were determined with respect to untreated controls unless otherwise noted. A P value less than .05 was considered significant. A log-rank test was performed between treatment groups for the Kaplan-Meier survival curve.

Results

Moderate Heating Nanosecond Pulse Stimulation is Cytotoxic to KLN205 Cells in a 3-D Cell Model

In a 3-D agarose cell-culture model, nanosecond pulses applied to KLN205 squamous cell carcinoma cells preheated to 43°C were more lethal than against cells pulsed at room temperature ($P < .001$), as indicated by a higher propidium iodide uptake in the heated condition (Figure 2D, F, H, J, and L). Significant propidium iodide uptake was not observed in the sham control nor when cells were exposed to heat alone without pulses (Figure 2A and B). In cells pulsed at room temperature (Figure 2C, E, G, I, and K), distinct propidium iodide uptake was not observed at an applied voltage of 150 V (Figure 2C) and was only observed around the high-voltage electrodes, not in the center of the applied field, in the 300 V condition (Figure 2E). Cell killing between the electrodes was observed starting at a dose of 600 V in cells pulsed at room temperature (Figure 2G). In contrast, though not significant, we observed cell killing within the electrode gap at the minimal dose of 150 V in cells preheated to 43°C (Figure 2D). This effect was linear with respect to increasing applied voltage, wherein a higher applied voltage yielded enhanced propidium iodide uptake and a higher fluorescence signal ($P < .001$; Figure 2M). The integrated fluorescence density was similar for cells preheated to 43°C and pulsed with 150 V to cells pulsed at room temperature with 750 V (Figure 2M).

Moderate Heating Nanosecond Pulse Stimulation Widens the Ablation Zone in a 3-D Cell Model

Following nanosecond pulse application, KLN205 cells in a 3-D model exhibited an ablation zone that widened as the applied

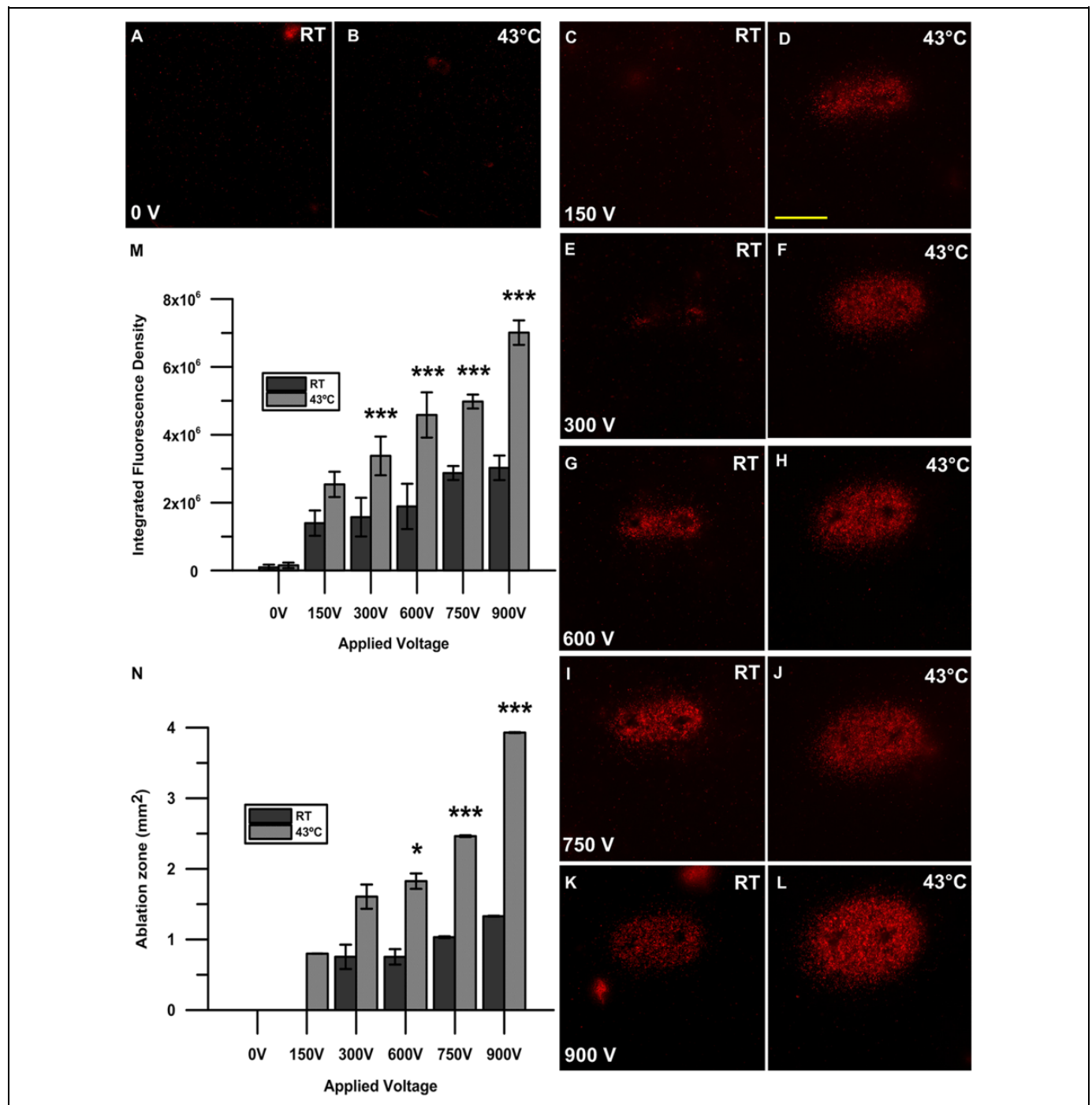


Figure 2. Propidium iodide uptake after nanosecond pulse stimulation with and without the application of moderate heat. A 2-needle electrode with a 1 mm gap was used to pulse KLN205 cells with 200, 300 ns pulses at 50 Hz with voltages of 150, 300, 600, 750, and 900 V at either room temperature (RT; C, E, G, I, K) or 43°C (D, F, H, J, L). A sham control (0 V) without pulses at RT (A) and 43°C (B) was also recorded. Micrographs are representative of 3 to 5 replicates per treatment group. Scale bar = 1 mm. Quantification of cell death after nanosecond pulse stimulation is represented as the integrated fluorescence density of each individual sample using ImageJ software to draw a region of interest around the area of fluorescence signal. Results shown are the mean of 3 to 5 replicates per group (standard deviation). *** $P < .001$ (M). The area of the ellipse-shaped ablation zone (mm²) was calculated by multiplying the semi-major and semi-minor axes indicative of propidium iodide uptake by π wherein $A = \pi ab$. The calculated area is shown as mm². Results shown are the mean of 3 to 5 replicates per group (\pm standard deviation). * $P < .05$, ** $P < .01$, *** $P < .001$ (N).

voltage was increased (Figure 2N). In cells that were pulsed at 43°C, this effect was more pronounced, with an elliptical-shaped ablation zone of 3.93 ± 0.50 mm² achieved with the

application of 900 V. This area was significant with respect to cells pulsed at room temperature with 900 V, where a maximal ablation zone of only 1.33 ± 0.01 mm² was reached ($P < .001$;

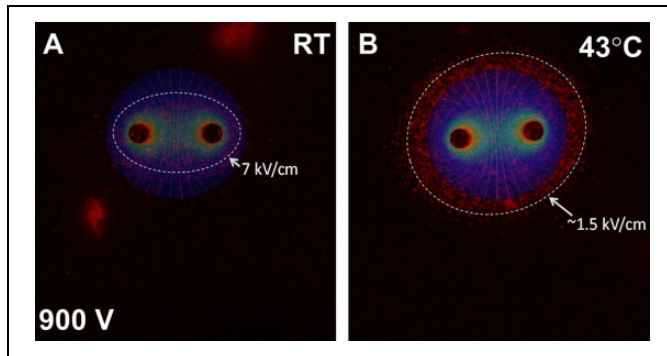


Figure 3. Two-dimensional electrostatic model of NPS with and without MH. Fluorescence micrograph indicating propidium iodide uptake after NPS with 200, 300 ns pulses at 50 Hz with 900 V at RT (A) and MH-NPS at 43°C (B) and overlaid electric field contour. Highest level of propidium iodide uptake was observed at an electric field strength of 7 kV/cm (A) and 1.5 kV/cm (B) for cells pulsed at RT and preheated to 43°C, respectively. MH-NPS indicates nanosecond pulse stimulation with moderate heating; RT, room temperature.

Figure 2N). Furthermore, at the minimal dose of 150 V, a distinct region of killing was not observed, though an ablation zone of $0.80 \pm 0.26 \text{ mm}^2$ resulted from cells pulsed at 43°C at the same voltage.

Electric Field of NPS Is Enhanced With Application of MH

In a 3-D agarose cell-culture model, nanosecond pulses applied to KLN205 squamous cell carcinoma cells preheated to 43°C were more lethal than against cells pulsed at room temperature as evidenced by higher propidium iodide uptake. Overlaid electric field diagram for cells pulsed at 900 V at room temperature where an electric field of 7 kV/cm was needed to achieve the size of the ablation zone (Figure 3A). By comparison, an overlaid electric field diagram for cells preheated to 43°C and pulsed at 900 V indicates that an electric field of approximately 1.5 kV/cm was needed to achieve the much larger size of the ablation zone (Figure 3B).

Tumor Ablation With NPS Is Enhanced With MH

Tumor growth or regression was recorded following treatment. Tumor growth was highest in the untreated tumors, in tumors treated with heat alone, and in tumors receiving 600, 100 ns pulses at 9.8 kV without heat (Figure 4A). No complete responses were observed in the aforementioned groups. Tumors treated with 21 kV or 15.4 kV with or without MH showed a significant tumor volume reduction from day 18 to day 63 compared to untreated controls ($P < .05$). Tumor regression was significant in tumors treated with 9.8 kV with MH starting from day 25 after treatment ($P < .05$). The marked reduction in tumor volume included a large percentage of complete regressions, particularly at the later time points. The largest difference between moderately heated and unheated pulsed tumors were those treated with 9.8 kV (Figure 4B).

Overall Survival Is Improved for Mice Treated With MH-NPS

Survival was significantly enhanced in tumors treated at 21 kV ($P < .001$), 15.4 kV + heat ($P < .001$), 15.4 kV ($P < .001$), and 9.8 kV + heat ($P < .01$) compared to untreated tumors (Figure 4C). At day 63 after treatment, mice receiving tumor-targeted pulses at 21 kV and 15.4 kV + heat exhibited the highest survival rates of 80% and 75%, respectively. Similarly, survival rates of 62.5% and 50% were observed in mice with tumors treated at 15.4 kV and 9.8 kV + heat in that order. Mice receiving 9.8 kV without heat were all euthanized due to clinical criteria, for example, excessive tumor burden or morbidity, at or before day 25, and similarly for animals dosed with heat alone by day 42. In the untreated controls, mortality was 100% by day 31. We did not observe a protective effect in any treatment group when the tumor-free mice were challenged with KLN205 cells on the opposite flank (Figure 4D).

Discussion

The current study indicates that MH-NPS can be used to ablate ectopic murine squamous cell carcinoma tumors. Thermal damage occurs as a function of increasing temperature and time of heating; therefore, our goal was to create a system for applying controlled MH in combination with NPS. Our electrode delivery system for MH-NPS achieves that.

To avoid heat-induced cell death, 43°C was chosen as the target temperature, as temperatures above 43°C have been shown to induce cell death.³³ The duration of MH at a target temperature of 43°C is approximately 2 minutes. Heating KLN205 carcinoma cells in a 3-D culture model did not cause cell death, and MH alone had minimal effect on *in vivo* tumor growth and no effect on survival. However, we observed a synergistic cytotoxic effect between MH and NPS in both a 3-D cell-culture model and with *in vivo* tumor regression. Additionally, MH-NPS significantly widened the ablation zone in a 3-D cell model, particularly in the region between the electrodes where the applied electric field is the weakest. The MH-NPS also enhanced overall survival *in vivo* compared to that of animals treated with NPS alone at the same voltage.

A possible explanation for the synergistic effect between MH and NPS is the increase in tumor conductivity, indicated by a large decrease in tumor impedance. Our group previously reported this phenomenon in a pancreatic cancer model using IRE protocols, wherein the actual dose of energy to the tumor was higher in tumors treated with both MH and IRE compared to those treated with IRE alone, resulting in enhanced tumor ablation.³¹ Using MH-NPS to treat squamous cell carcinoma, we see this same effect, where parallel treatments at the same voltage, with one including MH, improve the rate of tumor regression. Other groups have utilized laser heating for antitumor effects^{34,35} but not in combination with NPS.

In summation, with the addition of moderate heat, the applied voltage can be reduced to achieve the same treatment efficacy. Our results suggest a reduction of at least 27% in the

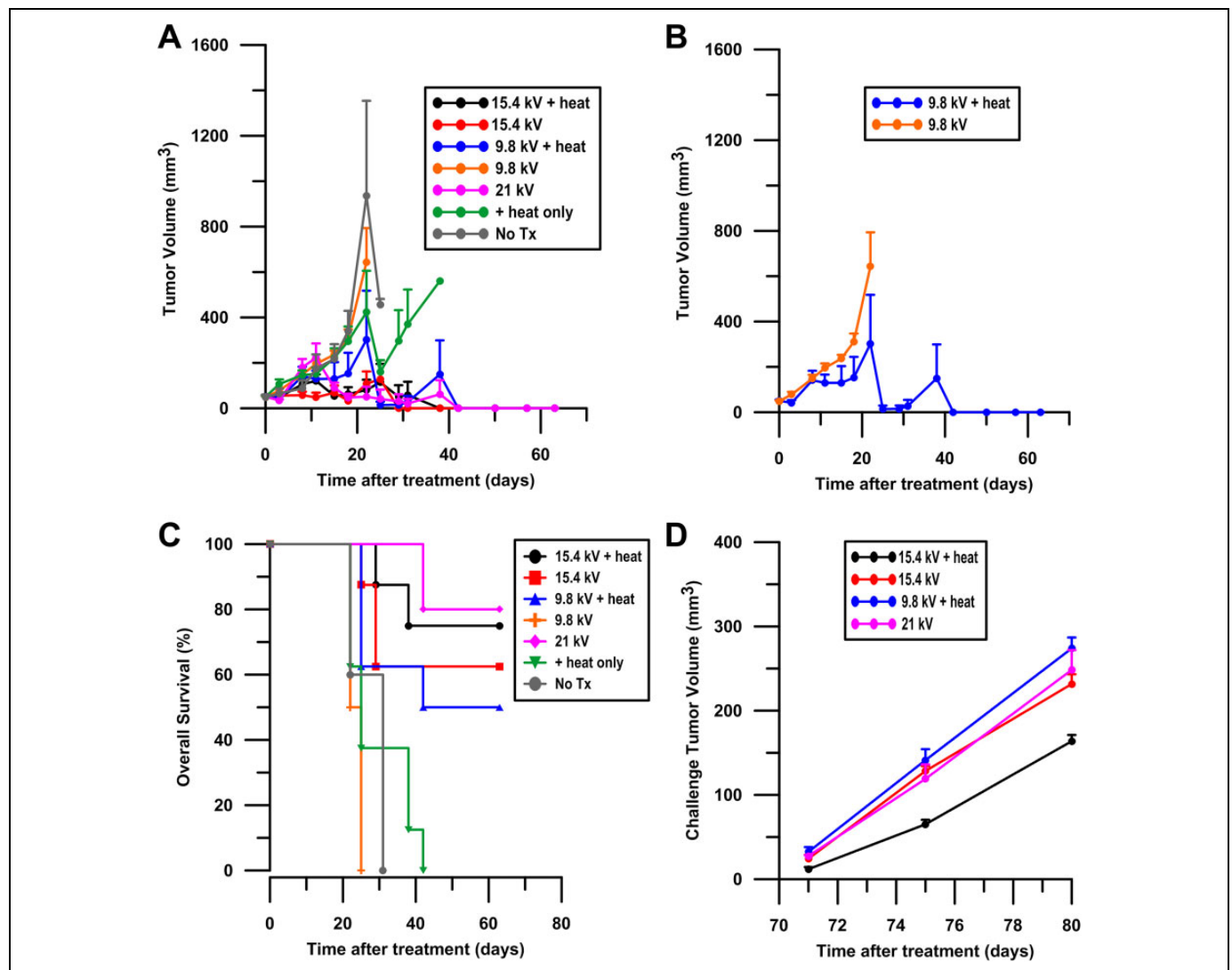


Figure 4. Tumor regression after MH-NPS. KLN205 ectopic murine squamous cell carcinoma tumors were given a single MH, NPS, or MH-NPS treatment on day 0 at an approximate size of 50 mm³. Tumor volume was recorded in surviving animals until day 63 (A). Groups include an untreated no treatment control (no Tx), tumors treated with heat alone, tumors pulsed at a voltage of 9.8 kV or 15.4 kV with and without the application of heat, and tumors pulsed at a voltage 21 kV. A total of 50 mice were used in this experiment. Results of 9.8 kV with and without heat are displayed separately to observe difference between tumors heated and not heated at that voltage (B). Results shown are the mean of 5 to 8 replicates per group (\pm standard error of the mean) at day 0. Sample size is lower at later time points due to euthanasia by clinical criteria. Kaplan-Meier survival curves are reported until the completion of the study at day 63 (C). A total of 50 mice were used for this experiment. All groups included 8 mice per treatment with the exception of the no treatment control (no Tx) and 21 kV groups, which each contained 5 animals. Mice tumor free at 63 days were challenged on the opposite flank with 5×10^5 KLN2015 cells. Challenge tumor volumes were recorded. Results shown are the mean of 4 to 6 tumor-free replicates per group (\pm standard error of the mean), as not all mice were tumor free by day 63 (D). MH-NPS indicates nanosecond pulse stimulation with moderate heating.

applied voltage (21 to 15.4 kV + heat) to achieve a similar level in both tumor regression and overall survival. In addition, at an even lower voltage, 9.8 kV, with MH-NPS, we observed a significant survival enhancement compared to untreated mice and those treated with NPS or MH alone, suggesting the voltage could be dropped by as much as 53% to obtain a similar level of tumor regression and to improve overall survival. This is an important finding considering the invasive nature of tumor resection and ablative surgeries and that high applied voltages are often associated with major complications.³ There

is also an equipment limitation. Higher applied voltages require a larger power supply, possibly multiple electrodes, and in general greater engineering support to achieve the desired dose. Therefore, using lower applied voltages is more feasible for both the patient and the clinician.

We do not propose MH-NPS to be an alternative thermal ablation platform. Current microwave and radiofrequency ablative therapies are most efficient for thermal ablation, where the goal is to raise the target tumor temperature to a lethal temperature, thereby inducing necrosis or apoptosis.³⁶ Instead,

our platform provides fast, focused MH (43°C) to the target tissue only; a benefit of utilizing a laser heating source versus microwaves³⁷⁻³⁹ or radiofrequency,^{6-8,36} whose temperatures can exceed 100°C and 150°C, respectively, and can in some cases stimulate heat-induced tumor spreading.⁴⁰ By combining low-voltage NPS with a moderate amount of heat, we can mitigate these deleterious effects providing high-power fast heating with an infrared laser. In the current study, we have demonstrated a synergy between heat-induced cell dilation and application of NPS, thereby enhancing the cytotoxic effects of NPS alone and avoid thermal damage or heat-induced cell death. The greatest effort will be to accommodate the treatment of larger tumors, specifically those with a diameter larger than 3 cm. This size limitation was indicated in clinical data from IRE ablation therapies.³ Penetration depth and variation in thermal properties of tissue are inherent physical challenges for clinical applications involving large tumors. Preliminary studies show that variation in heat absorption coefficients among tissues of the same thickness is relatively small compared to that in tissues of different thickness. Although tissue deep below the surface may receive less heating compared to the surface initially, heating the target for a period of time, for example, 3 minutes, could reduce the absorption coefficient at the surface and hence allow deeper penetration of the heating and treatment. More studies are in progress to determine the absorption coefficients and their dependence on tissue and temperature. In these complex cases, multiple lasers may be needed to achieve MH of larger targets. Data from our 3-D *in vitro* cell-culture model, where an ablation zone nearly 4 times larger than the area of the applied electric field was achieved, suggest we can treat larger tumors with modifications to electrode and laser configurations. Future work will focus on the effort to treat larger, orthotopic tumors of various cancer types with MH-NPS.

Acknowledgments

The authors would like to thank Claudia Muratori, PhD, for technical expertise in developing the 3-D cell-culture model, and the SoBran personnel who manage the vivarium facility at ODU.


Declaration of Conflicting Interests

The author(s) declared the following potential conflicts of interest with respect to the research, authorship, and/or publication of this article: With respect to duality of interest and financial disclosures, Drs K. Schoenbach and R. Heller are inventors on patents which cover the technology that was used in the work reported in this manuscript. In addition, Drs K. Schoenbach and R. Heller own stock in Pulse Biosciences, Inc.

Funding

The author(s) disclosed receipt of the following financial support for the research, authorship, and/or publication of this article: This research was supported by a grant award from Pulse Biosciences, Inc.

ORCID iD

Richard Heller, PhD  <http://orcid.org/0000-0003-1899-3859>

References

1. Que SKT, Zwald FO, Schmults CD. Cutaneous squamous cell carcinoma: incidence, risk factors, diagnosis, and staging. *J Am Acad Dermatol*. 2018;78(2):237-247.
2. van Meerbeeck JP, Fennell DA, De Ruysscher DK. Small-cell lung cancer. *Lancet*. 2011;378(9804):1741-1755.
3. Scheffer HJ, Nielsen K, de Jong MC, et al. Irreversible electroporation for nonthermal tumor ablation in the clinical setting: a systematic review of safety and efficacy. *J Vasc Interv Radiol*. 2014;25(7):997-1011; quiz 1011.
4. Jiang C, Davalos RV, Bischof JC. A review of basic to clinical studies of irreversible electroporation therapy. *IEEE Trans Biomed Eng*. 2015;62(1):4-20.
5. Paiella S, Butturini G, Frigerio I, et al. Safety and feasibility of irreversible electroporation (IRE) in patients with locally advanced pancreatic cancer: results of a prospective study. *Digest Surg*. 2015;32(2):90-97.
6. Zhang Y, Bergman JJ, Xue L, et al. Preliminary study on efficacy of radiofrequency ablation combined with endoscopic resection for eradicating widespread early non-flat type esophageal squamous cell carcinoma [in Chinese]. *Zhonghua Wei Chang Wai Ke Za Zhi*. 2015;18(9):875-880.
7. Baba Y, Watanabe M, Kawanaka K, et al. Radiofrequency ablation for pulmonary metastases from esophageal squamous cell carcinoma. *Dis Esophagus*. 2014;27(1):36-41.
8. Cash BD, Johnston LR, Johnston MH. Cryospray ablation (CSA) in the palliative treatment of squamous cell carcinoma of the esophagus. *World J Surg Oncol*. 2007;5:34.
9. Wust P, Hildebrandt B, Sreenivasa G, et al. Hyperthermia in combined treatment of cancer. *The Lancet. Oncology*. 2002;3(8):487-497.
10. Phillips MA, Narayan R, Padath T, Rubinsky B. Irreversible electroporation on the small intestine. *Br J Cancer*. 2012;106(3):490-495.
11. Onik G, Mikus P, Rubinsky B. Irreversible electroporation: implications for prostate ablation. *Technol Cancer Res T*. 2007;6(4):295-300.
12. Bower M, Sherwood L, Li Y, Martin R. Irreversible electroporation of the pancreas: definitive local therapy without systemic effects. *J Surg Oncol*. 2011;104(1):22-28.
13. Charpentier KP, Wolf F, Noble L, Winn B, Resnick M, Dupuy DE. Irreversible electroporation of the pancreas in swine: a pilot study. *HPB (Oxford)*. 2010;12(5):348-351.
14. Kwon D, McFarland K, Velanovich V, Martin RC II. Borderline and locally advanced pancreatic adenocarcinoma margin accentuation with intraoperative irreversible electroporation. *Surgery*. 2014;156(4):910-920.
15. Martin RCG II. Multi-disciplinary management of locally advanced pancreatic cancer with irreversible electroporation. *J Surg Oncol*. 2017;116(1):35-45.
16. Fruhling P, Nilsson A, Duraj F, Haglund U, Noren A. Single-center nonrandomized clinical trial to assess the safety and efficacy of irreversible electroporation (IRE) ablation of liver tumors in humans: short to mid-term results. *Eur J Surg Oncol*. 2017;43(4):751-757.

17. Langan RC, Goldman DA, D'Angelica MI, et al. Recurrence patterns following irreversible electroporation for hepatic malignancies. *J Surg Oncol*. 2017;115(6):704-710.
18. Beebe SJ, Fox PM, Rec LJ, Willis EL, Schoenbach KH. Nanosecond, high-intensity pulsed electric fields induce apoptosis in human cells. *FASEB J*. 2003;17(11):1493-1495.
19. Batista Napotnik T, Wu YH, Gundersen MA, Miklavcic D, Vernier PT. Nanosecond electric pulses cause mitochondrial membrane permeabilization in Jurkat cells. *Bioelectromagnetics*. 2012;33(3):257-264.
20. Semenov I, Xiao S, Pakhomova ON, Pakhomov AG. Recruitment of the intracellular Ca^{2+} by ultrashort electric stimuli: the impact of pulse duration. *Cell Calcium*. 2013;54(3):145-150.
21. Nuccitelli R, Pliquett U, Chen X, et al. Nanosecond pulsed electric fields cause melanomas to self-destruct. *Biochem Bioph Res Co*. 2006;343(2):351-360.
22. Chen R, Sain NM, Harlow KT, et al. A protective effect after clearance of orthotopic rat hepatocellular carcinoma by nanosecond pulsed electric fields. *Eur J Cancer*. 2014;50(15):2705-2713.
23. Chen X, Zhuang J, Kolb JF, Schoenbach KH, Beebe SJ. Long term survival of mice with hepatocellular carcinoma after pulse power ablation with nanosecond pulsed electric fields. *Technol Cancer Res T*. 2012;11(1):83-93.
24. Muratori C, Pakhomov AG, Heller L, et al. Electrosensitization increases antitumor effectiveness of nanosecond pulsed electric fields in vivo. *Technol Cancer Res T*. 2017;16(6):987-996.
25. Nuccitelli R, Wood R, Kreis M, et al. First-in-human trial of nanoelectroablation therapy for basal cell carcinoma: proof of method. *Exp Dermatol*. 2014;23(2):135-137.
26. Rossmanna C, Haemmerich D. Review of temperature dependence of thermal properties, dielectric properties, and perfusion of biological tissues at hyperthermic and ablation temperatures. *Crit Rev Biomed Eng*. 2014;42(6):467-492.
27. Kanduser M, Sentjurs M, Miklavcic D. The temperature effect during pulse application on cell membrane fluidity and permeabilization. *Bioelectrochemistry*. 2008;74(1):52-57.
28. Donate A, Bulysheva A, Edelblute C, et al. Thermal assisted in vivo gene electrotransfer. *Curr Gene Ther*. 2016;16(2):83-89.
29. Sarnaik AA, Sussman JJ, Ahmad SA, McIntyre BC, Lowy AM. Technology for the delivery of hyperthermic intraoperative intraperitoneal chemotherapy: a survey of techniques. *Recent Results Cancer Res*. 2007;169:75-82.
30. Muratori C, Pakhomov AG, Pakhomova ON. Effect of cooling on cell volume and viability after nanoelectroporation. *J Membrane Biol*. 2017;250(2):217-224.
31. Edelblute CM, Horneff J, Burcus NI, et al. Controllable moderate heating enhances the therapeutic efficacy of irreversible electroporation for pancreatic cancer. *Sci Rep*. 2017;7(1):11767.
32. Muratori C, Pakhomov AG, Xiao S, Pakhomova ON. Electrosensitization assists cell ablation by nanosecond pulsed electric field in 3D cultures. *Sci Rep*. 2016;6:23225.
33. Hildebrandt B, Wust P. The biologic rationale of hyperthermia. *Cancer Treat*. 2007;134:171-184.
34. Manuchehrabadi N, Chen Y, Lebrun A, Ma R, Zhu L. Computational simulation of temperature elevations in tumors using Monte Carlo method and comparison to experimental measurements in laser photothermal therapy. *J Biomed Eng*. 2013;135(12):121007.
35. Stureson C, Andersson-Engels S. A mathematical model for predicting the temperature distribution in laser-induced hyperthermia. Experimental evaluation and applications. *Phys Med Biol*. 1995;40(12):2037-2052.
36. Rhim H, Goldberg SN, Dodd GD, et al. Essential techniques for successful radio-frequency thermal ablation of malignant hepatic tumors. *Radiographics*. 2001;21:17-39.
37. Pearce JA, Cook JR, Emelianov SY. Ferrimagnetic nanoparticles enhance microwave heating for tumor hyperthermia therapy. *Conf Proc IEEE Eng Med Biol Soc*. 2010; 2010:2751-2754.
38. Heerink WJ, Solouki AM, Vliegenthart R, et al. The relationship between applied energy and ablation zone volume in patients with hepatocellular carcinoma and colorectal liver metastasis. *Eur Radiol*. 2018;28(8):3228-3236. doi:10.1007/s00330-017-5266-1.
39. De Cobelli F, Marra P, Ratti F, et al. Microwave ablation of liver malignancies: comparison of effects and early outcomes of percutaneous and intraoperative approaches with different liver conditions: new advances in interventional oncology: state of the art. *Med Oncol*. 2017;34(4):49.
40. Velez E, Goldberg SN, Kumar G, et al. Hepatic thermal ablation: effect of device and heating parameters on local tissue reactions and distant tumor growth. *Radiology*. 2016;281(3):782-792.